Density dependence buffers natural populations against multiple stressors

Man Qi[1,2*], Àlex Giménez Romero[1,3], Jiamiao Chen[2], Qianzhao Sun[4], Tao Sun[4], Roberto Salguero-Gómez[1]

1. Department of Biology, University of Oxford, 11a Mansfield Rd, Oxford OX1 3SZ, UK.

2 Key laboratory of Geographical Process Analysis & Simulation of Hubei Province/College of Urban and Environmental Sciences, Central China Normal University, Wuhan 430079, China.

3. Theoretical and Computational Ecology Group, CEAB (CSIC), Blanes, Catalonia, Spain.

4. State Key Laboratory of Wetland Conservation and Restoration, School of Environment, Beijing Normal University, Beijing, 100875, China

* Corresponding author: Man Qi (man.qi@biology.ox.ac.uk)

Open research statement: Data and code for the *Suaeda salsa* experiment can be found at https://github.com/ManQiEcology/Dataset-and-code-for-Density-dependence-buffers-natural-populations-against-multiple-stressors. The code of the IBM model can be found at https://github.com/agimenezromero/plant-growth-model/.

Summary (171 out of 200 words)

Predicting population persistence under global change requires understanding how populations buffer against interacting stresses. Gradual stresses, such as droughts, suppress individual performance, whereas abrupt stresses, such as harvesting, remove individuals from populations. Because these stresses interact through density-dependent responses of growth, reproduction and survival, predicting their combined effects requires understanding density dependence processes. Here, we introduce a mechanistic framework linking individual-level density dependence to population buffering by integrating the constant final yield rule, self-thinning, and the hydra effect. Using field experiments and individual-based modelling of the annual marsh plant *Suaeda salsa*, we show that gradual stress suppresses individual growth, weakens competition and reduces population buffering against abrupt disturbances. Consequently, synergistic interactions between gradual and abrupt stresses become increasingly likely as population density declines or gradual stress intensifies. We further show that the slope of the relationship between body mass and population density provides a robust indicator for population buffering. Our framework offers a powerful tool to understand and predict population persistence under multiple interacting stresses.

Introduction (549 words)

Global change is exposing natural populations to multiple interacting stresses[1,2], while making it increasingly difficult to predict population persistence. External stresses

42 influence the dynamics of populations through two distinct pathways: stresses either
43 progressively suppress individual performance[3-7] or abruptly remove individuals from
44 the population[6]. Indeed, stressors such as droughts, warming, and inundation primarily
45 reduce individual growth, reproduction, and survival over time[3-7] (hereafter, 'gradual
46 stresses'), whereas herbivory, predation, and harvesting primarily act by removing
47 individuals[6] (hereafter, 'abrupt stresses').

48 Natural populations are rarely exposed to a single stress[1,2]. For example, drought and
49 herbivory jointly cause salt marsh dieback[8]. Similarly, climate change and poaching
50 accelerate the decline of succulent plants[9] and rhinos[10] in South Africa. More broadly,
51 a meta-analysis showed that gradual and abrupt stresses (referred to as physical and
52 consumer control in the original paper[11]) can interact antagonistically, additively, or
53 synergistically across ecosystems. Yet, what determines when each type of stress
54 interaction emerges remains unknown.

55 Negative density dependence is a fundamental mechanism that stabilizes populations
56 and promotes their persistence[12-16]. Yet, density-dependence remains underrepresented
57 in demographic models[17]. This is because explicitly parameterizing density-dependent
58 models requires intensive individual-level data spanning a wide range of population
59 densities[18]. Consequently, we still lack a general, mechanistic understanding of how
60 density dependence generates population buffering under multiple stresses[19].

61 Population buffering too can arise via density dependence[20]. For instance, negative
62 density dependence of vital rates (*e.g.*, growth, reproduction, survival) can compensate

63 population biomass loss caused by density independent mortality[13,21-24]. To develop a
64 mechanistic understanding of how density dependence generates population buffering,
65 we unify three classic but historically separate concepts into a single mechanistic
66 framework. The three key concepts are the constant final yield rule[25], self-thinning
67 rule[26], and the hydra effect[14,21]. Although developed independently, these concepts
68 together describe successive density-dependent responses of growth, reproduction, and
69 survival along a continuous population-density gradient, as explained below.

70 Intraspecific competition generates density-dependent responses in vital rates, which in
71 turn determine the capacity of populations to buffer against density loss. At low
72 population densities, competition is weak and individuals grow and reproduce largely
73 independently of density[27]. As density increases, competition progressively suppresses
74 growth and/or reproduction[19,27], producing the constant final yield[25]. At still higher
75 densities, competition increases mortality, leading to self-thinning[26]. Conversely, when
76 abrupt stresses reduce population density, competition is relaxed, allowing
77 compensatory increases in growth[13], reproduction[21,22], and survival[23,24] of surviving
78 individuals. Under certain conditions, overcompensation in reproduction and/or
79 survival can even increase subsequent population size following abrupt stress, giving
80 rise to the hydra effect[14].

81 Our mechanistic framework yields five testable predictions about how gradual stresses
82 reshape population buffering. Because gradual stresses suppress individual
83 performance[28], we first hypothesise that (H1) gradual stresses primarily reduce

84 individual growth. As growth suppression delays the onset of population crowding[29],
85 we further hypothesise that (H2) gradual stresses reduce the intensity of intraspecific
86 competition. Because negative density dependence arises from intraspecific
87 competition, weakened competition should reduce compensatory responses of growth,
88 reproduction, and survival following abrupt stresses. We therefore hypothesise that (H3)
89 gradual stresses weaken population buffering against abrupt stresses. Consequently, we
90 hypothesise that (H4) the interaction between gradual and abrupt stresses shifts from
91 antagonistic to additive and ultimately synergistic as population density decreases
92 and/or gradual stress intensifies. Finally, we hypothesise that (H5) the slope of the log-
93 transformed relationship between body mass and population density provides a robust
94 indicator of population buffering, with steeper slopes reflecting stronger density
95 dependence and greater compensatory capacity. We test these predictions using field
96 experiments and individual-based modelling of the annual marsh plant *Suaeda salsa*
97 (Amaranthaceae).

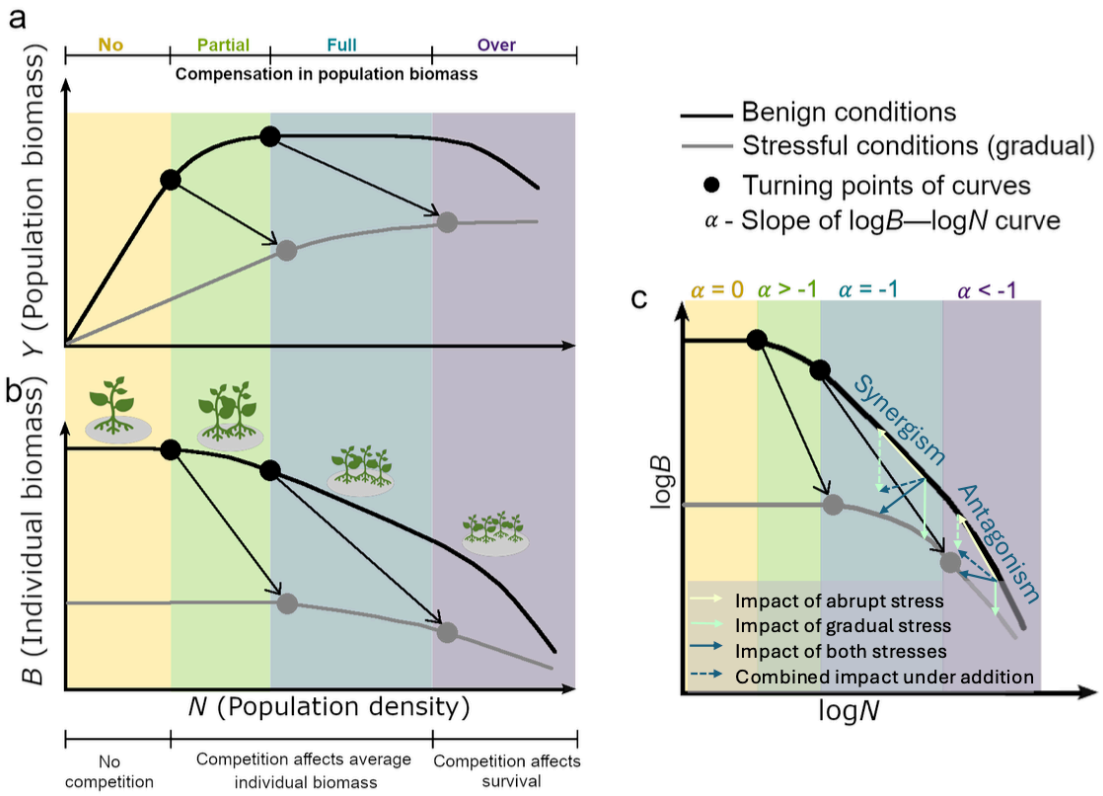


Figure 1. Framework illustrating how population buffering declines as population density decreases and gradual stress intensifies. (**a, b**) Under benign conditions (black curves), population biomass (*Y*) initially increases linearly with population density (*N*), then saturates, and may decline as competition progressively suppresses individual vital rates of growth, reproduction, and ultimately survival. Following an abrupt stress (*e.g.,* harvesting, consumption), compensatory responses of vital rates buffer population biomass to different degrees depending on the initial population density: no compensation (yellow zone), partial compensation (green zone), full compensation (blue zone), and overcompensation (purple zone). Gradual stress (grey curves; *e.g.*, drought, inundation) suppresses individual performance and weakens competition, shifting turning points rightward and narrowing the range of population densities over which compensation occurs. (**c**) The log*B*-log*N* relationship

between mean individual biomass (B) and population density (N). The slope (α) of this relationship ($\log B$-$\log N$) reflects the strength of density dependence and compensation of population biomass such that: $\alpha = 0$ indicates no compensation, $-1 < \alpha < 0$ partial compensation, $\alpha = -1$ full compensation (*i.e.,* constant final yield [25]), and $\alpha < -1$ overcompensation, where self-thinning[26] or the hydra effect[14,21] may occur. Coloured zones are defined under benign conditions and shift under gradual stress, as indicated by the displacement of the curve turning points. Coloured solid arrows indicate the individual effects of gradual stress (green), abrupt stress (yellow), and their combined effect (blue). Dashed arrows indicate the expected impact if the two stresses act additively. Panels **a** and **b** were adapted from Beaugendre et al[27].

Results (954 words)

Experimental responses of Suaeda salsa to gradual and abrupt stresses

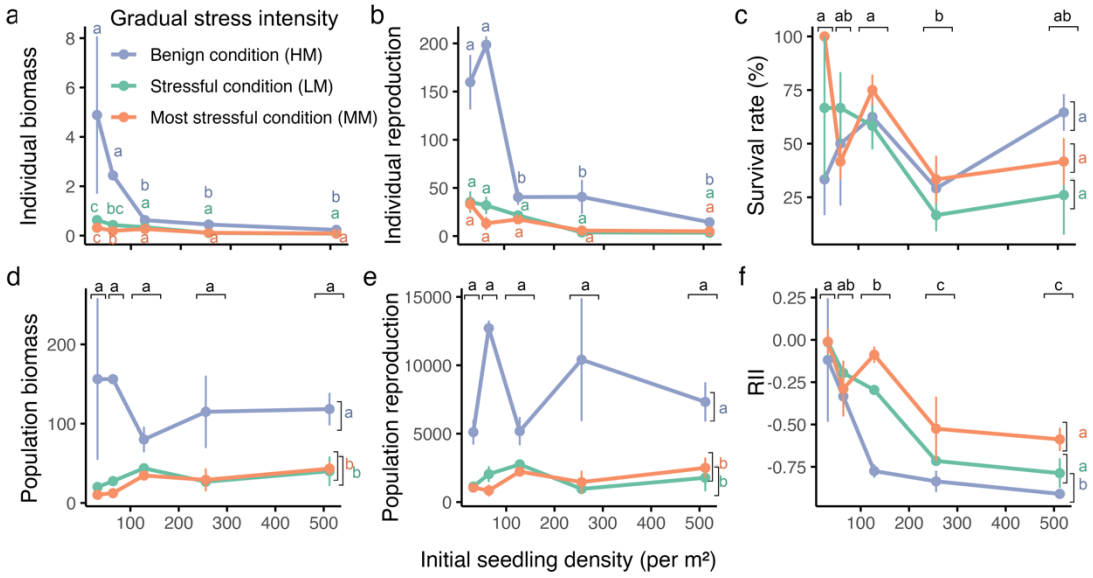
We tested the predictions of our framework using a field experiment that manipulated initial seedling density of the annual plant species *Suaeda salsa* across three marsh zones in the Yellow River Delta, China. Seedling density was manipulated to mimic crab herbivory (*Helice tientsinensis*), an abrupt stress that removes seedlings during early spring (Fig. S1a), whereas the low-, mid-, and high-marsh zones represented a gradient of gradual stress in flooding frequency and soil salinity[30]. We used the maximum individual size attained by *S. salsa* in each marsh zone (Fig. S2a–c) to classify stress intensity, with high marsh being exposed to 'benign conditions', low marsh being 'stressful conditions', and mid marsh as 'most stressful conditions'. To

quantify the intensity of intraspecific competition in our experiment, we used the Relative Interaction Index (*RII*[31]), where negative values indicate competition and positive values indicate facilitation. We used this experiment to test the aforementioned hypotheses H1–H3 and H5.

Consistent with H1, gradual stress primarily suppressed individual growth. Compared with plants in the benign conditions (*i.e.*, high marsh), individuals in the stressful conditions (*i.e.*, low marsh) and most stressful conditions (*i.e.*, mid marsh) have lower end-of-season biomass ($F_{2,28} = 24.02$, $p < 0.001$, Fig. 2a), height ($F_{2,27} = 19.86$, $p < 0.001$, Fig. S2a), width ($F_{2,27} = 55.2$, $p < 0.001$, Fig. S2b), and tiller number ($F_{2,27} = 39.52$, $p < 0.001$, Fig. S2c), indicating a consistent reduction in individual growth under increasing stress. Reproduction is likewise lower in stressful and most stressful conditions ($F_{2,28} = 89.08$, $p < 0.001$, Fig. 2b). In contrast, survival does not differ significantly among marsh zones ($F_{2,30} = 0.79$, $p = 0.46$, Fig. 2c), suggesting that gradual stress primarily reduce growth and reproduction rather than survival within the density range here examined.

We find support for H2, where we had expected gradual stress to weaken intraspecific competition. *RII* values indicate weaker competition in stressful and most stressful conditions than in benign conditions ($F_{2,28} = 14.94$, $p < 0.001$, Fig. 2f). The weaker competition in stressful and most stressful conditions can be explained by the overall smaller size (Fig. S2a-c) and lower biomass (Fig. 2a) of individual survived in these conditions. which indicate less canopy overlap and crowding

Providing support for H3, we find that gradual stresses weaken compensatory responses of vital rates to density reduction, thereby reducing population buffering. Within the population density range manipulated in our experiment, compensation is observed primarily through growth and reproduction, whereas survival shows little response to density reduction (Fig. S2d). This result may reflect the experimental density range not reaching the self-thinning region, where density-dependent responses in survival are expected to emerge (see Discussion). Under benign conditions (high marsh), reducing initial plant density significantly increases individual height ($F_{4,27} = 3.96$, $p = 0.012$, Fig. S2a), width ($F_{4,27} = 12.08$, $p < 0.001$, Fig. S2b), tiller number ($F_{4,27} = 6.99$, $p < 0.001$, Fig. S2c), individual biomass ($F_{4,28} = 19.69$, $p < 0.001$, Fig. 2a), and reproduction ($F_{4,28} = 36.389$, $p < 0.001$, Fig. 2b). These compensatory responses weaken under stressful (low marsh) and most stressful conditions (mid marshes) (Fig. 2a, b; Fig. S2a-c). Although individual growth and reproduction respond strongly to population density, population biomass and seed production varied little across the experimental density gradient (Fig. 2d,e). The contrasting responses observed at the individual and population levels indicate that compensatory responses of vital rates buffer populations against abrupt stress. Together, these results support H3 by showing that gradual stresses weaken population buffering through reduced compensatory responses of vital rates.

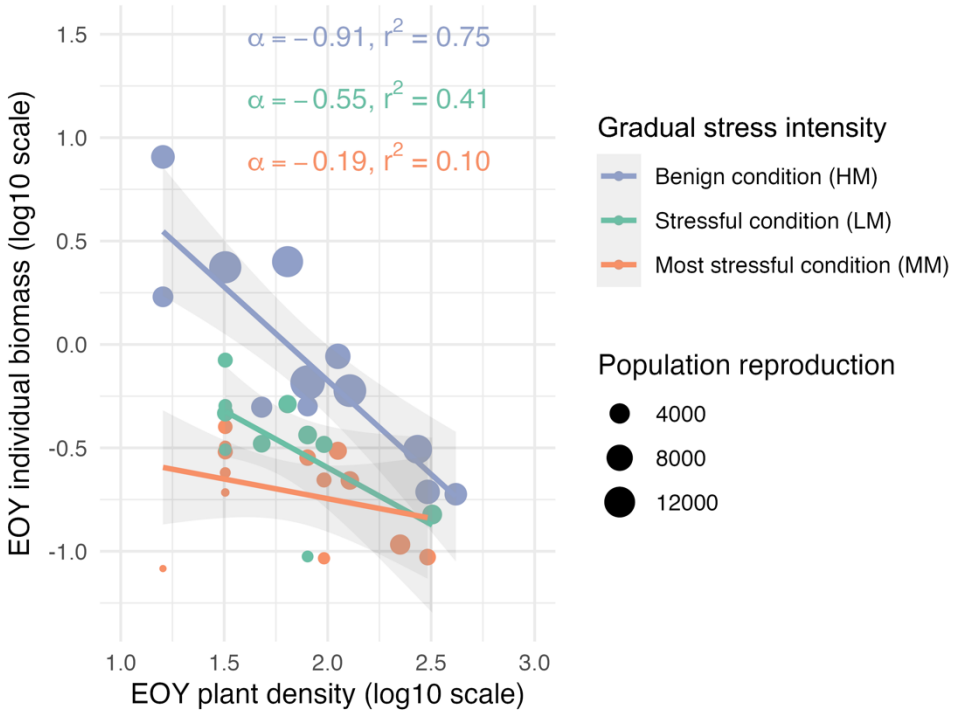


172

173 **Figure 2. Gradual stress weakens compensatory responses of vital rates to density**
174 **reduction, reducing population buffering. (a, b)** Individual biomass (g) and
175 reproduction (seeds per plant) increased as initial seedling density decreased, with the
176 strongest compensatory responses in benign conditions (*i.e.*, high marsh, HM). These
177 responses weakened in the stressful (low marsh, LM) and most stressful (mid marsh,
178 MM) conditions. **(c)** Survival showed only weak responses to reduction in population
179 density across different intensity of gradual stress. **(d, e)** Despite strong density-
180 dependent responses of individual biomass and reproduction, population biomass and
181 seed production remained largely unchanged across the experimental density gradient.
182 **(f)** Intraspecific competition, measured by the Relative Interaction Index (RII),
183 weakened from the benign conditions to stressful and most stressful conditions. More
184 negative RII values indicate stronger competition. Error bars indicate standard errors.
185 Different letters indicate significant differences ($p < 0.05$). For panels with a significant
186 gradual stress × population density interaction (panels a, b), letters denote pairwise
187 comparisons of initial seedling density treatments under a given level of gradual stress.

For panels without a significant interaction (panels c-f), letters indicate differences among main effects (gradual stress or density).

In consistence with H5, the slope of the relationship between body mass and population density (log$B$–log$N$) reflect the strength of population buffering against abrupt stress. In benign conditions, the slope of the log$B$–log$N$ relationship ($\alpha = -0.91 \pm 0.17$ S.E.) is not significantly different from that predicted by the constant final yield rule ($\alpha = -1$; $t = 0.56$, $p > 0.5$), indicating nearly complete compensation of population biomass following density reduction (Fig. 3). The slope becomes progressively shallower in the stressful ($\alpha = -0.55 \pm 0.23$ S.E.) and the most stressful ($\alpha = -0.19 \pm 0.18$ S.E.) conditions, indicating weaker compensatory responses under increasing gradual stress. The slope differs significantly between benign conditions and the most stressful conditions ($p = 0.0053$), whereas the difference between the benign conditions and stressful conditions is not significant ($p = 0.24$). Together, these results support H5 by showing that shallower log$B$–log$N$ relationships result in weaker density dependence and reduced population buffering.



203

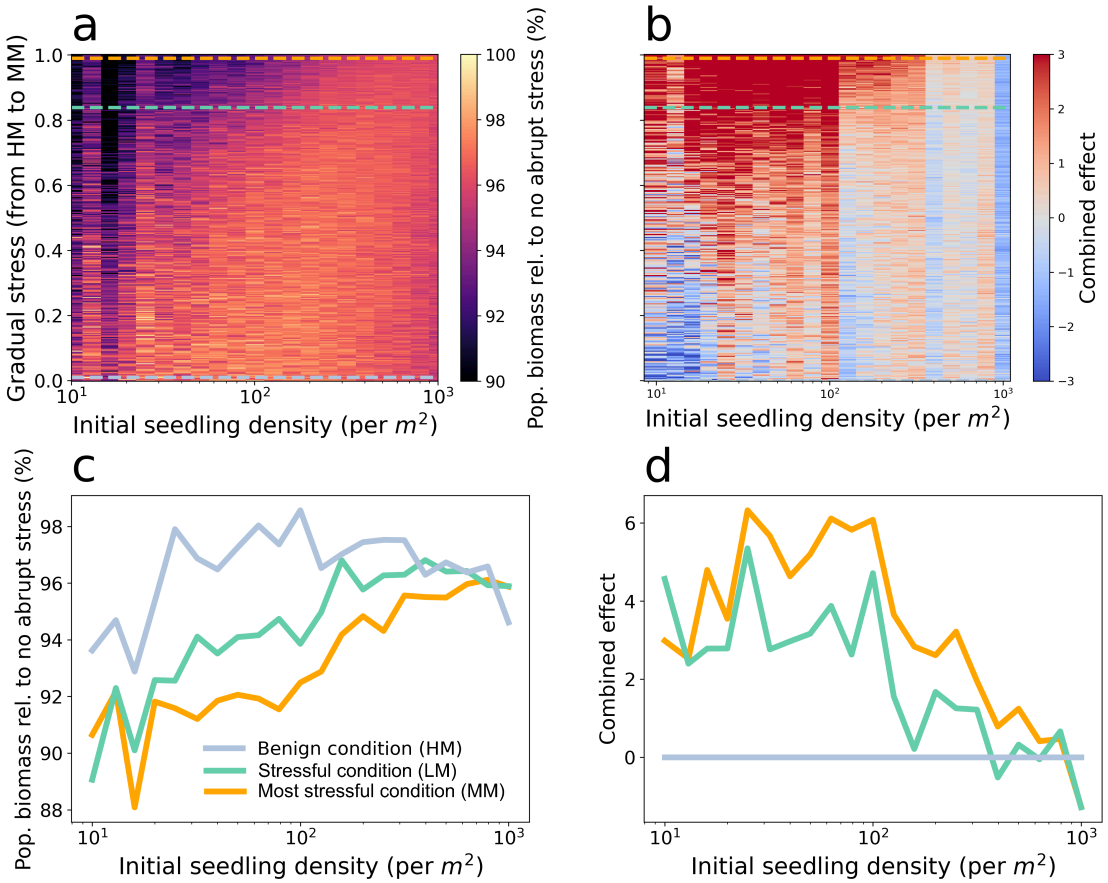
204 **Figure 3. The slope of the relationship between body mass and population**
205 **density(log*B*–log*N*) reflects the strength of density dependence and the**
206 **corresponding capacity for population buffering.** At the end of the growing season,
207 the average individual biomass (g) of *Suaeda salsa* was plotted against population
208 density (individuals/m^2) for each quadrat. Linear regressions were fitted to the observed
209 log*B*–log*N* relationships at each level of gradual stress. Shallower regression slopes
210 indicate weaker compensatory responses of end-of-year (EOY) individual biomass to
211 density reduction under increasing stress. Point size is proportional to population seed
212 production (seeds/m^2).

213 *Combined effects of gradual and abrupt stresses*

214 Although the findings from the *S. salsa* field experiment supported our hypotheses H1–
215 H3 and H5, our experimental design (see Methods) sampled only a discrete range of

population densities and gradual stress levels. To test our expectation in H4 that interactions between gradual and abrupt stresses shift from antagonistic to additive and ultimately synergistic as population density decreases and/or gradual stress intensifies, we developed a spatially explicit individual-based model (IBM) for *S. salsa* parameterized with our field data. The model simulates individual growth, resource competition, and population dynamics across continuous gradients of population density and gradual stress over a 120-day growing season (see Methods for details). We parameterized the IBM using the abovementioned experimental results in benign, stressful, and most stressful conditions. The IBM successfully reproduced both the observed log$B$–log$N$ relationships (Fig. S3a) and the compensatory recovery of population biomass following abrupt stress (Fig. 4b), indicating that the model captured the essential density-dependent processes observed in the field.

The IBM simulations support H4 that interaction between gradual and abrupt stresses shifted from antagonistic to additive and ultimately synergistic as population density decreased and gradual stress intensified (Fig. 4b,d). With abrupt stress held constant (10% plant removal), the reduction in end-of-season population biomass increases as population density decreased and gradual stress intensified (Fig. 4a,c), indicating progressively weaker population buffering. Consequently, synergistic interactions dominates under low population density and high gradual stress, whereas additive and antagonistic interactions emerge under higher population density and weaker gradual stress (Fig. 4b, d). Together, these simulations support H4 by showing that interaction types shift predictably as population density decreases and gradual stress intensifies.



238

239 **Figure 4. Individual-based model predicts that gradual stress weakens population**
240 **buffering and shifts interactions between gradual and abrupt stresses.** A spatially
241 explicit individual-based model (IBM), parameterized using field data of *Suaeda salsa*,
242 simulated individual growth over a growing season as a function of intrinsic growth
243 rate (representing gradual stress intensity) and competition for resources among
244 neighbouring plants with overlapping canopies. **(a)** End-of-year population biomass
245 under abrupt stress relative to undisturbed populations. Population buffering weakens
246 as population density decreases and gradual stress intensified. **(b)** Combined effects of
247 gradual and abrupt stresses shift predictably along the density gradient, from
248 antagonistic at high density to synergistic at low density as gradual stress intensified.
249 **(c, d)** Cross-sections of panels **a** and **b** comparing benign condition (HM), stressful

condition (LM) and most stressful condition (MM), showing weaker population buffering (**c**) and stronger synergistic interactions (**d**) under greater gradual stress. Combined effects were calculated as the deviation from the additive expectation (see Methods).

Discussion (1008 words)

Density dependence is a fundamental mechanism through which local populations buffer environmental pertubations[12-16]. Yet, how density dependence and corresponding population buffering changes under multiple interacting stresses has remained poorly understood. Here we show that gradual stresses can weaken density dependence and its associated potential for population buffering, thereby shifting interactions between gradual and abrupt stresses from antagonistic to additive and ultimately synergistic as population density decreases. By integrating the historically disconnected concepts of the constant final yield rule[25], self-thinning rule[26], and the hydra effect[14,21] into a single mechanistic framework, we explain how density-dependent responses of vital rates can generate population buffering and why this buffering weakens under gradual stress. Together, our framework provides a predictive basis for understanding and predicting population persistence under multiple interacting stresses.

Negative density dependence is widely recognized as a key mechanism promoting population stability by reducing population growth at high population densities and relaxing competitive constraints at low densities[20]. At the level of individual vital rates,

this stability emerges through compensatory responses in growth, reproduction, and survival that buffer populations against density loss[13,21-24]. Although population buffering can arise through multiple local mechanisms[20], empirical demonstrations of buffering mediated by density dependence have largely relied on long-term, individual-based studies of a few species[16,18], limiting the development of a general mechanistic understanding. Here, by integrating gradual and abrupt stresses with density dependence and population buffering, our framework extends these species-specific observations into a general, testable explanation of how compensatory responses emerge and why they weaken under gradual stress.

A key contribution of our framework is its conceptual integration of the constant final yield rule, self-thinning, and the hydra effect into a continuous sequence of compensatory responses to density reduction. Demographic models typically describe density dependence separately for individual vital rates[32,33]. Our study instead suggests that density dependence can be expressed sequentially through different vital rates as competition intensifies along the population-density gradient[19,27]. From this perspective, the constant final yield rule, self-thinning, and the hydra effect represent successive stages of the same density-dependent process rather than independent ecological phenomena. One implication of this framework is that apparent differences in the vital rates exhibiting density dependence may partly reflect the range of population densities sampled rather than different forms of density dependence. This interpretation is illustrated by two studies of the same Soay sheep (*Ovis aries*) population, in which negative density dependence in adult male survival emerged only after the sampled

density range was extended to higher population sizes[34,35]. Similarly, experimental studies in plants show that individual growth and morphology often respond more strongly and across a broader portion of the density gradient than survival, which typically exhibits substantial declines only under more intense competition associated with self-thinning[36].

Our findings highlight the importance of rethinking how the combined effects of multiple stresses in natural populations have been historically interpreted. Rather than representing fixed properties of particular stress pairs[2,11], antagonistic, additive, and synergistic interactions emerge from the population's position along the density gradient and the strength of gradual stress (Fig. 4). As gradual stress weakens compensatory responses of vital rates, populations lose their capacity to buffer density loss caused by abrupt stress, making synergistic interactions increasingly likely. Conversely, stronger density dependence at higher population densities maintains greater buffering capacity, resulting in additive or antagonistic interactions[37]. This mechanistic interpretation provides a general explanation for why the same pair of stressors can produce different interaction types across populations, environments, or stages of population development.

A practical advantage of our framework is that it identifies the slope of the relationship between individual body mass (B) and population density (N) ($\log B$–$\log N$) as an indicator of population buffering (Fig. 3). Rather than estimating density dependence separately for individual vital rates from long-term demographic

314 monitoring[34,38], the log$B$–log$N$ relationship captures their integrated consequences for
315 population buffering. Because mean individual biomass and population density are
316 comparatively straightforward to measure, changes in the slope can provide a
317 practical means of tracking shifts in population buffering under changing
318 environmental conditions. This approach may therefore complement demographic
319 analyses in systems where long-term individual-based monitoring is unavailable,
320 while providing a useful indicator for adaptive management under global change[14,19].

321 Our study also identifies several directions for extending this framework. Both the
322 field experiment and IBM primarily tested the portion of the density gradient over
323 which density dependence operated in the Yellow River Delta through growth and
324 reproduction. The limited response of survival likely reflects that the experimental
325 density range did not extend into the self-thinning region, where density-dependent
326 mortality is expected to emerge. The density range used in our field experiment
327 encompassed the typical seedling densities observed in *S. salsa* populations in the
328 Yellow River Delta[39] and was comparable to those reported for other temperate
329 coastal marshes[40,41]. Extending experimental and modelling approaches to encompass
330 this region will provide a direct test of whether gradual stress similarly weakens
331 density-dependent survival.

332 More generally, density-dependent responses of vital rates are likely to vary among
333 life-history stages (see [34,38]). Therefore, applying the framework to species with
334 overlapping generations and more complex life histories will help determine how the

sequence of density-dependent responses varies among life stages and demographic strategies. To do so, repeated measurements of growth, survival and reproduction across life-history stages should be integrated with mechanistic models that explicitly represent both resource competition among individuals and the allocation of acquired resources among growth, maintenance and reproduction within individuals. Existing frameworks, such as dynamic energy budget models coupled with integral projection models, provide one promising example of how these processes can be linked to population dynamics[42].

Our study shows that gradual stresses weaken density dependence and the associated population buffering, thereby altering how populations respond to interacting stresses. By integrating the constant final yield rule, self-thinning, and the hydra effect into a single mechanistic framework, we provide a general explanation for how compensatory responses of vital rates emerge and why they weaken under gradual stress. As global change increasing the co-occurrence of stressors[1,8], incorporating density-dependent mechanisms of population buffering into ecological theory and population models will improve our ability to understand and predict population persistence.

Online methods

Field experiment on Suaeda salsa in the Yellow River Delta

Study area To test H1-3 and H5, we conducted a field experiment in the Yellow River Delta National Natural Reserve, China (37°35′–38°12′ N, 118°33′–119°20′ E). In this region, the annual halophyte *Suaeda salsa* (Amaranthaceae) dominates intertidal

marshes[43]. Along the marsh elevation gradient, flooding frequency decreases upslope, whereas soil salinity peaks in the mid marsh because of high evapotranspiration and reduced tidal inundation[30]. Consequently, *S. salsa* experience contrasting levels of gradual stress across marsh zones. Periodic marsh diebacks triggered by the combined effect of spring drought (*i.e.*, gradual stress) and crab herbivory (*i.e.*, abrupt stress)[8,44], making this system well suited for testing our framework. Crab herbivory primarily removes seedling during early spring (see Appendix S1 for crab grazing causing *S. salsa* mortality) before stems become lignified and resistant to grazing. Therefore, we mimicked abrupt stress by manipulating initial seedling density in both the field experiment and the individual-based model.

Experiment design To test how gradual stress modifies density-dependent population buffering, we established a factorial field experiment manipulating (1) marsh zone, representing different levels of gradual stress, and (2) initial seedling density, representing different intensities of abrupt stress. In May 2022, we selected three marsh zones (high, low, and mid marsh) and established one 50 × 50 m^2 plot within each zone. Within each plot, we randomly established fifteen 25 × 25 cm^2 quadrats, spaced at least 2 m apart. Initial seedling density was adjusted to 2, 4, 8, 16, or 32 individuals per quadrat by removing surplus seedlings, with three replicate quadrats per density treatment. To prevent further crab grazing throughout the growing season, we excavated each quadrat to a depth of 20 cm, enclosed the intact soil block in 0.5 cm mesh netting, and reinstalled it with the mesh extending 20 cm above the soil surface. The mesh was supported by metal stakes.

Measurements Throughout the growing season (May–September 2022), we monitored plant growth and survival monthly. Growth was quantified as the height, canopy width, and tiller number of the five tallest individuals in each quadrat. At the end of the growing season (September), all above-ground biomass within each quadrat was harvested to quantify total population biomass and seed production. Mean individual biomass and seed production were calculated by dividing total population biomass and seed production by the number of surviving individuals in each quadrat.

Intraspecific competition To quantify the intensity of intraspecific competition (H2), we calculated the Relative Interaction Index (RII)[31]: $RII = (B_w - B_{ref}) / (B_w + B_{ref})$. There, B_w is the mean individual biomass within a quadrat. B_{ref} is the mean individual biomass in the lowest-density treatment (two initial seedlings per quadrat), representing the closest approximation to neighbour-free growth. RII ranges from −1 (strong competition) to +1 (strong facilitation). Because individuals grown in complete isolation were not included in the experimental design, RII should be interpreted as a conservative estimate of interaction strength.

Individual-based competition model

The individual-based competition model (IBM) was developed to test H4 by extending the field experiment across continuous gradients of population density and gradual stress that could not be achieved experimentally.

Model overview We developed a spatially explicit individual-based model to simulate *Suaeda salsa* individuals growing and competing for resources over a 120-day

399 growing season (May–September). Each individual was represented by a circular
400 crown centred on a fixed stem location, with a time-dependent radius describing both
401 plant size and the spatial extent of resource acquisition. Following zone-of-influence
402 models of plant competition[45,46], resource uptake decreased with distance from the stem,
403 and overlapping resource-acquisition zones generated local competition. Daily growth
404 depended on the resources acquired and was constrained by a logistic function limiting
405 plant size to a maximum radius (r_{max}), which represented the effect of gradual stress.
406 The model represents density dependence operating through competition-mediated
407 growth and does not explicitly include density-dependent mortality (self-thinning).
408 Consequently, it captures the growth component of the proposed framework but not the
409 survival component.

410 *Environment* We represented the environment as a square 100 × 100 cm^2 domain,
411 corresponding to 1m^2, with periodic boundary conditions. We discretized the domain
412 into resource cells with a spatial resolution of Δx = 1 cm. At the beginning of each daily
413 time step, we distributed a fixed total resource pool （R_{tot} =5×10^5） uniformly among
414 all resource cells. Individuals then removed resources from cells within their resource-
415 acquisition zones. At the end of each time step, we restored the resource field to its
416 initial homogeneous state, representing resource renewal between successive days and
417 preventing cumulative depletion across the growing season.

418 *Plant representation* We represented each plant *i* by its spatial coordinates (x_i, y_i),
419 its time- dependent radius $r_i(t)$, and a condition-specific maximum radius r_{max}. All

420 individuals started with radius r_0 = 1 cm, and their stem locations remained fixed
421 throughout the simulation. The current radius $r_i(t)$ defined both individual size and the
422 radius of the circular zone from which the plant acquired resources.

423 We described the decrease in resource uptake with distance using the coefficient

424 $$\alpha_i(t) = -\frac{ln\,(\epsilon)}{r_i(t)} \quad (1)$$

425 where ϵ = 0.9 was the fraction of maximum uptake occurring at the edge of the
426 resource-acquisition zone. Thus, $exp[-\alpha_i(t)r_i(t)] = \epsilon$, and the relative shape of the
427 uptake kernel remained constant as the plant grew.

428 Each plant was also characterised by a resource-unlimited growth coefficient σ,
429 the resources acquired during the current time step $R_i(t)$, and the maximum resources
430 it could acquire at its current size in the absence of competitors, $R_{i,\max}(t)$.

431 *Competition and resource uptake* At each daily time step, we calculated the
432 resources acquired by individual *i* as

433 $$R_i(t) = \sum_{j:d_{ij}<r_i(t)} R_j(t)exp\left[-\alpha_i(t)d_{ij}\right] \quad (2)$$

434 where d_{ij} was the periodic Euclidean distance between the stem of individual *i* and
435 resource cell *j*, and $R_j(t)$ was the resource availability in that cell. The sum was taken
436 over all cells within the current plant radius $r_i(t)$. Resources acquired by an individual
437 were removed from the corresponding cells, so individuals with overlapping resource-
438 acquisition zones competed for the locally available resource pool.

For each individual, we also calculated the maximum resources obtainable in the absence of competition as

$$R_{i,\max}(t) = \sum_{j:d_{ij}<r_i(t)} R_{j,0} exp\left[-\alpha_i(r) d_{ij}\right] \quad (3)$$

where $R_{j,0}$ was the resource availability in cell j immediately after homogeneous replenishment. We updated plant radius using the resource-limited logistic growth equation

$$r_i(t+1) = r_i(t) + \sigma(r_{\max}) min\left(1, \frac{R_i(t)}{R_{i,\max}(t)}\right) r_i(t) \left(1 - \frac{r_i(t)}{r_{\max}}\right) \quad (4)$$

The ratio $R_i(t)/R_{i,\max}(t)$ quantified the fraction of the resources available in the absence of competition that was acquired by individual i. Growth therefore approached the resource-unlimited rate when competition was weak and declined as neighbouring plants depleted locally available resources. The logistic term constrained individual size as $r_i(t)$ approached $r_{\max}$.

Initialization and simulation At the beginning of each simulation, we placed individuals independently and uniformly at random within the spatial domain. We precomputed the periodic distances between each plant stem and all resource cells. We then simulated 120 daily time steps. During each time step, we: (1) calculated resource acquisition and removed the corresponding resources from the environment; (2) updated individual radii according to Eq. (4); (3) restored the homogeneous resource field; and (4) recalculated $R_{i,\max}$ and α_i using each individual's updated radius.

458 We performed 50 independent spatial realisations for each combination of initial
459 population density and gradual-stress intensity and calculated population-level outputs
460 from the means across realisations. We implemented the model in Julia.

461 *Disturbance and scenario design* We simulated herbivory-like abrupt stress by
462 removing 10% of individuals on day 30. Removed individuals had their radii set to zero
463 and were excluded from subsequent resource acquisition and growth.

464 We assumed that individual biomass scaled with squared plant radius:

465 $$b_i(t) = \kappa r_i(t)^2 \quad (5)$$

466 where κ was the radius-to-biomass conversion coefficient. Total population biomass
467 at time t was therefore,

468 $$B(t) = \kappa \sum_{i \in \mathcal{L}(t)} r_i(t)^2 \quad (6)$$

469 where $\mathcal{L}(t)$ is the set of living individuals. Accordingly, the biomass removed by the
470 abrupt stress was

471 $$B_{rem} = \kappa \sum_{i \in \mathcal{R}} r_i(t_{\text{dist}})^2 \quad (7)$$

472 where $\mathcal{R}$ is the set of removed individuals and $t_{\text{dist}} = 30$ is the time at which de
473 disturbance occurs. We varied initial population density from 10 to 1000 seedlings/m^2
474 and gradual stress intensity from the benign high-marsh condition to the stressful low-
475 marsh condition (different $r_{\max}$ values). For each combination of stress and initial

density, we simulated populations with and without the removal of 10% of individuals (abrupt stress).

Parameterisation We parameterized the model using the observed relationships between log- transformed mean individual biomass and log-transformed population density in the high- and low-marsh zones of the Yellow River Delta (Fig. S3a). We represented gradual stress through its effect on the maximum attainable plant radius. We used $r_{max}^{HM} = 27.4$ cm for the benign high-marsh condition and $r_{max}^{LM} = 14.0$ cm for the stressful low-marsh condition, based on maximum plant sizes observed in the corresponding field conditions. We represented intermediate levels of gradual stress using intermediate values of r_{max}.

For each value of r_{max}, we calibrated the resource-unlimited growth coefficient σ so that an isolated plant starting at r_0 reached 95% of its condition-specific maximum radius after t_{cal} = 90 days:

$$\sigma(r_{max}) = -\frac{1}{t_{cal}} ln\left[\frac{r_0(1-\eta)}{\eta(r_{max}-r_0)}\right] \quad (8)$$

where η=0.95. This calibration maintained the same relative developmental timescale across gradual-stress scenarios while allowing maximum plant size to vary. All remaining ecological and spatial model parameters were held constant.

For comparison with observed biomass, we used radius-to-biomass conversion coefficients of κ_{HM} = 0.006 and κ_{LM} = 0.004 for the high- and low-marsh conditions, respectively. For the scenario analysis, we used κ = 0.005. Because the effects of

abrupt stress were expressed relative to the corresponding undisturbed simulation, this conversion coefficient cancelled from the calculated ratios and did not influence the estimated buffering or interaction effects.

We quantified population buffering as the end-of-season population biomass under abrupt stress relative to that in the corresponding simulation without abrupt stress:

$$P(g,N) = 100\frac{\overline{B_{g,a}}(T,N)}{\overline{B_{g,0}}(T,N)} \quad (9)$$

where $T = 120$ days, g denoted gradual-stress intensity, N was initial population density, a denoted the abrupt-stress treatment, 0 denoted the undisturbed treatment, and the overbar indicated the mean across spatial realisations. Values close to 100% indicated strong compensation for the biomass loss caused by abrupt stress.

We expressed the proportional effect of abrupt stress as

$$E_a(g,N) = 100 - P(g,N) = 100\left[1 - \frac{\overline{B_{g,a}}(T,N)}{\overline{B_{g,0}}(T,N)}\right] \quad (10)$$

To determine whether gradual stress alter the impact of abrupt stress, we calculated the combined effect as

$$I(g,N) = E_a(g,N) - E_a(0,N) \quad (11)$$

where $Ea(0,N)$ was the proportional effect of abrupt stress under the benign high-marsh condition at the same initial population density. Positive values indicated that gradual stress amplified the proportional biomass loss caused by abrupt stress (synergism),

values of zero indicated no interaction on this scale, and negative values indicated that gradual stress reduced the proportional effect of abrupt stress (antagonism).

IBM analyses For each combination of gradual stress and initial population density, we averaged outputs across 50 independent spatial realizations. Population buffering and interaction effects were calculated according to Eqs. (9–11), and visualized across continuous gradients of gradual stress and population density.

Statistical analyses

Experimental data To test the effects of gradual stress, initial seedling density, and their interaction on plant growth, reproduction, survival, and intraspecific competition (H1–H3), we used two-way analyses of variance (ANOVA). Response variables included plant height, canopy width, tiller number, individual biomass, individual seed production, survival rate, total population biomass, total seed production, and the Relative Interaction Index (*RII*). Gradual stress level (*i.e.*, marsh zone) and initial seedling density were treated as fixed factors. Model residuals were assessed for normality using the Shapiro–Wilk test. When necessary, response variables were log-transformed. If normality assumptions remained violated, we used aligned rank transform (ART[47]) models for non-parametric factorial ANOVA (see Table S1 for specific transformation made for each response variable to meet model assumptions). Significant interactions were followed by pairwise comparisons of estimated marginal means (EMMs) within each gradual stress level.

LogB–logN relationships To test H5, we fitted linear models with log10-transformed mean individual biomass (log*B*) as the response variable and log10-transformed population density (log*N*), physical stress level, and their interaction as predictors. The interaction term tested whether slopes differed among physical stress levels. To determine whether the slope in the benign conditions differed from that predicted by the constant final yield rule, we performed a two-sided *t*-test of the null hypothesis $\beta_1 = -1$ using the estimated regression coefficient and its standard error.

All statistical analyses were conducted in R v4.3.2[48].

Acknowledgements

This study was supported by National Natural Science Foundation of China (42306192). We thank F. Cao for help during fieldwork and the Yellow River Delta National Nature Reserve Management Committee for granting access to field sites. MQ was supported by a MSCA fellowship (EP/Z00232X/1) hosted by RSG. RSG was supported by a NERC Pushing the Frontiers grant (NE/X013766/1).

References

1 He, Q. & Silliman, B. R. Climate Change, Human Impacts, and Coastal Ecosystems in the Anthropocene. *Current Biology* **29**, R1021-R1035, doi:10.1016/j.cub.2019.08.042 (2019).

2 Rodríguez-Caro, R. C. *et al.* Synergistic and Additive Effects of Multiple Threats Erode Phylogenetic and Life History Strategy Diversity in Testudines and Crocodilia. *Ecology Letters* **28**, e70147, doi:https://doi.org/10.1111/ele.70147 (2025).

555 3 Kearney, W. S., Fernandes, A. & Fagherazzi, S. Sea-level rise and storm surges structure coastal
556 forests into persistence and regeneration niches. *PLOS ONE* **14**, e0215977,
557 doi:10.1371/journal.pone.0215977 (2019).
558 4 Serrano, O., Arias-Ortiz, A., Duarte, C. M., Kendrick, G. A. & Lavery, P. S. in *Ecosystem*
559 *Collapse and Climate Change* (eds Josep G. Canadell & Robert B. Jackson) 345-364
560 (Springer International Publishing, 2021).
561 5 Sanchez-Martinez, P. *et al.* Amazon rainforest adjusts to long-term experimental drought.
562 *Nature Ecology & Evolution*, doi:10.1038/s41559-025-02702-x (2025).
563 6 IUCN. The IUCN Red List of Threatened Species. (2020).
564 7 WWF. Living Planet Report 2024 – A System in Peril. (Gland, Switzerland, 2024).
565 8 He, Q., Silliman, B. R., Liu, Z. & Cui, B. Natural enemies govern ecosystem resilience in the
566 face of extreme droughts. *Ecology Letters* **20**, 194-201, doi:https://doi.org/10.1111/ele.12721
567 (2017).
568 9 Engelen, A., Davis, K., Ellis, A. G. & Salguero-Gómez, R. Poaching exacerbates the effects of
569 climate change on the long-term viability of an endemic South African succulent plant species.
570 *bioRxiv*, 2025.2001. 2020.633962 (2025).
571 10 Nhleko, Z. N., Ahrens, R., Ferreira, S. M. & McCleery, R. A. Poaching is directly and indirectly
572 driving the decline of South Africa's large population of white rhinos. *Animal Conservation* **25**,
573 151-163, doi:https://doi.org/10.1111/acv.12720 (2022).
574 11 Silliman, B. R. & He, Q. Physical Stress, Consumer Control, and New Theory in Ecology.
575 *Trends in Ecology & Evolution* **33**, 492-503, doi:https://doi.org/10.1016/j.tree.2018.04.015
576 (2018).

12 Knape, J. & de Valpine, P. Are patterns of density dependence in the Global Population Dynamics Database driven by uncertainty about population abundance? *Ecology Letters* **15**, 17-23, doi:https://doi.org/10.1111/j.1461-0248.2011.01702.x (2012).

13 Petraitis, P. S. The Role of Growth in Maintaining Spatial Dominance by Mussels (Mytilus Edulis). *Ecology* **76**, 1337-1346, doi:https://doi.org/10.2307/1940940 (1995).

14 Abrams, P. A. When does greater mortality increase population size? The long history and diverse mechanisms underlying the hydra effect. *Ecology Letters* **12**, 462-474, doi:https://doi.org/10.1111/j.1461-0248.2009.01282.x (2009).

15 Scholl, J. P., Urbina-Casanova, R. & Iler, A. M. The importance of negative density dependence for rare species persistence. *Biol Conserv* **274**, 109729, doi:https://doi.org/10.1016/j.biocon.2022.109729 (2022).

16 Milles, A. *et al.* Local buffer mechanisms for population persistence. *Trends in Ecology & Evolution* **38**, 1051-1059, doi:https://doi.org/10.1016/j.tree.2023.06.006 (2023).

17 Hernández, C. M., Stott, I., Koons, D. N. & Salguero-Gómez, R. Density dependence impacts our understanding of population resilience. *The American Naturalist*, doi:10.1086/739605 (2025).

18 Mugabo, M., Perret, S., Legendre, S. & Le Galliard, J.-F. Density-dependent life history and the dynamics of small populations. *Journal of Animal Ecology* **82**, 1227-1239, doi:https://doi.org/10.1111/1365-2656.12109 (2013).

19 Mrad, A. *et al.* Recovering the Metabolic, Self-Thinning, and Constant Final Yield Rules in Mono-Specific Stands. *Frontiers in Forests and Global Change* **3**, 62, doi:10.3389/ffgc.2020.00062 (2020).

20 Milles, A. *et al.* Local buffer mechanisms for population persistence. *Trends in Ecology & Evolution*, doi:10.1016/j.tree.2023.06.006.

21 Ricker, W. E. Stock and Recruitment. *Journal of the Fisheries Research Board of Canada* **11**, 559-623, doi:10.1139/f54-039 (1954).

22 Ozgul, A., Fichtel, C., Paniw, M. & Kappeler, P. M. Destabilizing effect of climate change on the persistence of a short-lived primate. *Proceedings of the National Academy of Sciences* **120**, e2214244120, doi:doi:10.1073/pnas.2214244120 (2023).

23 Boyce, M. S. & Merrill, E. H. Compensation and density dependence. *PeerJ PrePrints*, doi:https://doi.org/10.7287/peerj.preprints.1944v1 (2016).

24 Clark, J. S. Density-independent mortality, density compensation, gap formation, and self-thinning in plant populations. *Theoretical Population Biology* **42**, 172-198, doi:https://doi.org/10.1016/0040-5809(92)90011-H (1992).

25 Harper, J. *Population biology of plants*. (Academic Press, 1977).

26 Yoda, K. Self-thinning in overcrowded pure stands under cultivated and natural conditions (Intraspecific competition among higher plants. XI). *Journal of Biology* **14**, 107-129 (1963).

27 Beaugendre, A., Mingeot, D. & Visser, M. Complex plant interactions in heterogeneous material require the ecological rethinking of sowing density recommendations for bread wheat. A review. *Agronomy for Sustainable Development* **42**, 9, doi:10.1007/s13593-021-00735-7 (2022).

28 Lakshmanan, P. & Robinson, N. in *Sugarcane: Physiology, Biochemistry, and Functional Biology* 411-434 (2013).

29 Stadt, K. J., Taylor, G. J. & Dale, M. R. T. Measuring the effect of an abiotic stress on competition. *Oecologia* **100**, 221-228, doi:10.1007/BF00316948 (1994).

30 Qi, M. *et al.* Maintenance of salt barrens inhibited landward invasion of Spartina species in salt marshes. *Ecosphere* **8**, doi:10.1002/ecs2.1982 (2017).

31 Armas, C., Ordiales, R. & Pugnaire, F. I. MEASURING PLANT INTERACTIONS: A NEW COMPARATIVE INDEX. *Ecology* **85**, 2682-2686, doi:https://doi.org/10.1890/03-0650 (2004).

32 Hernández, C. M., Stott, I., Koons, D. N. & Salguero-Gómez, R. Density Dependence Impacts Our Understanding of Population Resilience. *The American Naturalist* **207**, 693-709, doi:doi:10.1086/739605 (2026).

33 Hodgson, E. E., Essington, T. E. & Halpern, B. S. Density dependence governs when population responses to multiple stressors are magnified or mitigated. *Ecology* **98**, 2673-2683, doi:https://doi.org/10.1002/ecy.1961 (2017).

34 Coulson, T. *et al.* Age, sex, density, winter weather, and population crashes in Soay sheep. *Science* **292**, 1528-1531, doi:10.1126/science.292.5521.1528 (2001).

35 Milner, J. M., Elston, D. A. & Albon, S. D. Estimating the contributions of population density and climatic fluctuations to interannual variation in survival of Soay sheep. *Journal of Animal Ecology* **68**, 1235-1247, doi:https://doi.org/10.1046/j.1365-2656.1999.00366.x (1999).

36 Tessier, M., Gloaguen, J. C. & Lefeuvre, J. C. Influence of biotic and abiotic factors on the morphology and reproduction of Suaeda maritima on a salt marsh. *C R Acad Sci III* **323**, 905-911, doi:10.1016/s0764-4469(00)01233-6 (2000).

37 Raimondo, S. Density dependent functional forms drive compensation in populations exposed to stressors. *Ecological Modelling* **265**, 149-157, doi:https://doi.org/10.1016/j.ecolmodel.2013.06.014 (2013).

38 van Benthem, K. J. *et al.* Trait–demography relationships underlying small mammal population

fluctuations. *Journal of Animal Ecology* **86**, 348-358, doi:https://doi.org/10.1111/1365-2656.12627 (2017).

39 Qiu, D. *et al.* Reciprocal facilitation between annual plants and burrowing crabs: Implications for the restoration of degraded saltmarshes. *Journal of Ecology* **109**, 1828-1841, doi:https://doi.org/10.1111/1365-2745.13608 (2021).

40 Chaisson, C., Jones, C. C. & Warren, R. S. Seasonal Stem Loss and Self-thinning in Low Marsh Spartina alterniflora in a New England Tidal Marsh. *Estuaries and Coasts* **45**, 2102-2111, doi:10.1007/s12237-022-01054-0 (2022).

41 Liu, W. & Pennings, S. C. Self-thinning and size-dependent flowering of the grass Spartina alterniflora across space and time. *Functional Ecology* **33**, 1830-1841, doi:https://doi.org/10.1111/1365-2435.13384 (2019).

42 Smallegange, I. M., Caswell, H., Toorians, M. E. & de Roos, A. M. Mechanistic description of population dynamics using dynamic energy budget theory incorporated into integral projection models. *Methods in Ecology and Evolution* **8**, 146-154 (2017).

43 Qi, M. *et al.* Competitive ability, stress tolerance and plant interactions along stress gradients. *Ecology* **99**, 848-857, doi:10.1002/ecy.2147 (2018).

44 Zhang, L. *et al.* Interactive effects of crab herbivory and spring drought on a Phragmites australis-dominated salt marsh in the Yellow River Delta. *Science of The Total Environment* **766**, 144254, doi:https://doi.org/10.1016/j.scitotenv.2020.144254 (2021).

45 Casper, B. B., Schenk, H. J. & Jackson, R. B. DEFINING A PLANT'S BELOWGROUND ZONE OF INFLUENCE. *Ecology* **84**, 2313-2321, doi:https://doi.org/10.1890/02-0287 (2003).

46 Weiner, J., Stoll, P., Muller-Landau, H., Jasentuliyana, A. & null, n. The Effects of Density,

Spatial Pattern, and Competitive Symmetry on Size Variation in Simulated Plant Populations. *The American Naturalist* **158**, 438-450, doi:10.1086/321988 (2001).

47 Wobbrock, J. O., Findlater, L., Gergle, D. & Higgins, J. J. in *Proceedings of the SIGCHI Conference on Human Factors in Computing Systems* 143–146 (Association for Computing Machinery, Vancouver, BC, Canada, 2011).

48 Team, R. C. (R Foundation for Statistical Computing, Vienna, Austria, 2024).

Supplement

Density dependence buffers natural populations against multiple stressors

Man Qi[1,2*], Àlex Giménez Romero[1,3], Jiamiao Chen[2], Qianzhao Sun[4], Tao Sun[4], Roberto Salguero-Gómez[1]

1. Department of Biology, University of Oxford, 11a Mansfield Rd, Oxford OX1 3SZ, UK.

2 Key laboratory of Geographical Process Analysis & Simulation of Hubei Province/College of Urban and Environmental Sciences, Central China Normal University, Wuhan 430079, China.

3. Theoretical and Computational Ecology Group, CEAB (CSIC), Blanes, Catalonia, Spain.

4. State Key Laboratory of Wetland Conservation and Restoration, School of Environment, Beijing Normal University, Beijing, 100875, China

* Corresponding author: Man Qi (man.qi@biology.ox.ac.uk)



Figure. S1 (**a**) Crab grazing caused mortality of *Suaeda salsa* seedlings in spring, 2022. (**b**) *Suaeda salsa* has high plasticity of size as indicated from individuals collected on the same day across the marsh in July 2022. Photo credit: Man Qi.

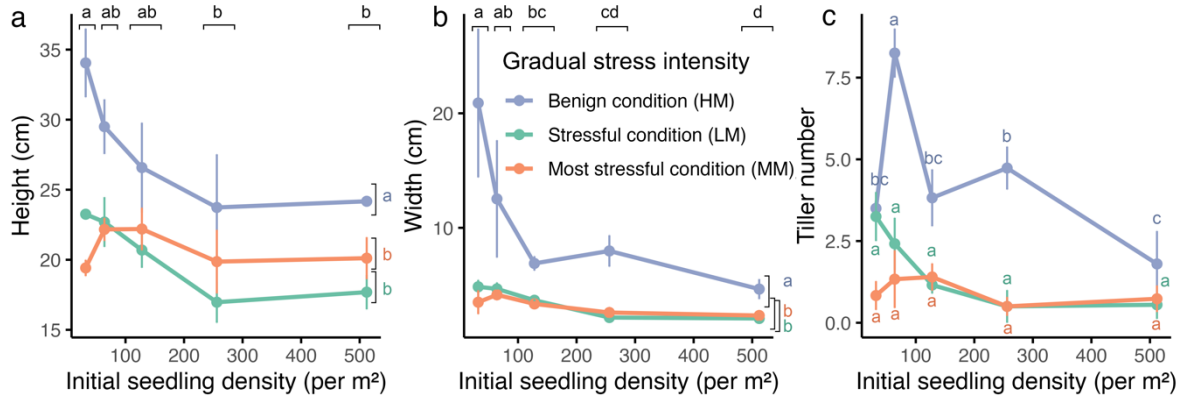


Figure S2. Gradual stress suppresses individual growth and weakens density-dependent compensatory growth. Panels show (**a**) maximum plant height ($F_{2,27} = 19.86$, $p < 0.001$ for gradual stress, $F_{4,27} = 3.96$, $p = 0.012$ for initial seedling density, no significant interaction between gradual stress and initial seedling density), (**b**) maximum width ($F_{2,27} = 55.2$, $p < 0.001$ for gradual stress, $F_{4,27} = 12.08$, $p < 0.001$ for initial seedling density, no significant interaction), and (**c**) maximum tiller number ($F_{2,27} = 39.52$, $p < 0.001$ for gradual stress, $F_{4,27} = 6.99$, $p < 0.001$ for initial seedling density, significant interaction) of *Suaeda salsa* (mean ± SE) across five initial seedling densities and three gradual stress intensities (HM-high marsh; MM-mid marsh; LM-low marsh). Different letters indicate significant differences at $p < 0.05$. For panels

with a significant gradual stress × population density interaction (panel c), letters denote pairwise comparisons of density treatments within each marsh zone. For panels without a significant interaction (c), letters indicate differences based on main effects (gradual stress intensity or population density).

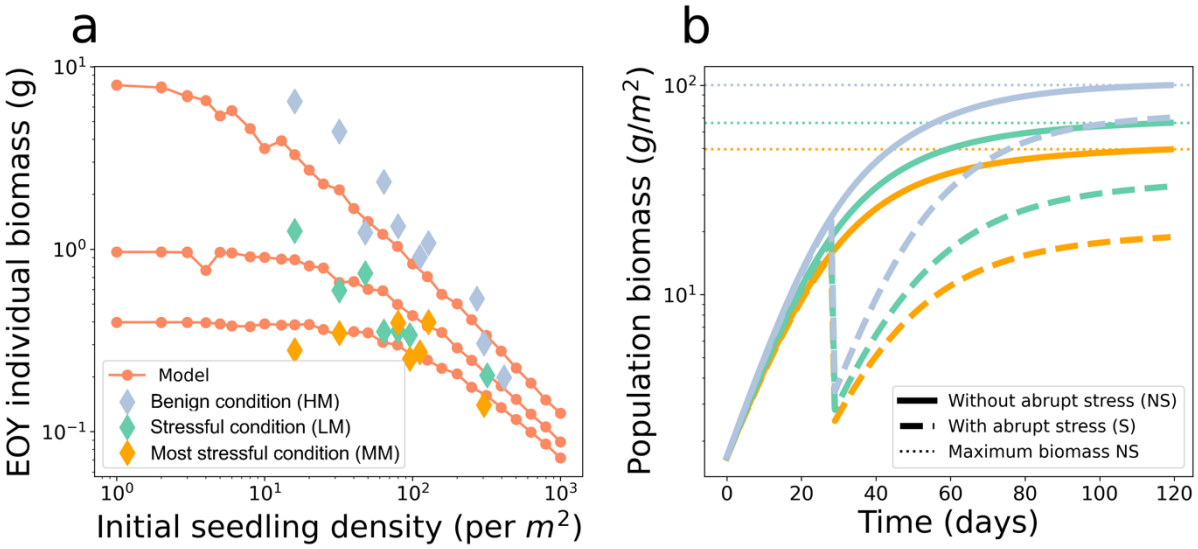


Figure S3. The individual-based model reproduces the observed density-dependent growth responses and stronger population buffering under benign than stressful conditions. (**a**) The model reproduced the observed log-transformed end of year (EOY) mean individual biomass–density relationship from the benign condition (here high marsh-HM), stressful condition (low marsh-LM), and most stressful condition (mid marsh-MM) in *Suaeda salsa* experiment. (**b**) Simulated abrupt stress (*i.e.*, early-season removal of 10% of plants) produced stronger population biomass compensation under benign conditions than under stressful conditions.

Table S1. Summary of two-way ANOVA and aligned rank transform (ART) results for the effect of marsh zone (*Zone*), initial plant density treatment (*Density*), and their interaction on plant performance metrics. The table indicates whether log transformation or ART was applied to meet model assumptions. Degrees of freedom (DF), F-values, and

associated *p*-values are reported. Significance levels are denoted as follows: $p > 0.05$ (ns), $p < 0.05$ (*), $p < 0.01$ (**), $p < 0.001$ (***).

Response Variable	Transformation	Factor	DF	F-value	P-value	Significance
Height (cm)	None	Zone	2, 27	19.86	4.97E-06	***
		Density	4, 27	3.96	0.0119	*
		Zone × Density	8, 27	1.34	0.2675	ns
Width (cm)	Log	Zone	2, 27	55.2	2.89E-10	***
		Density	4, 27	12.08	9.33E-06	***
		Zone × Density	8, 27	2.28	0.0520	ns
Tiller number	None	Zone	2, 27	38.52	1.23E-08	***
		Density	4, 27	6.99	5.37E-04	***
		Zone × Density	8, 27	3.97	0.0032	**
Individual biomass	ART	Zone	2, 28	24.02	8.42E-07	***
		Density	4, 28	19.69	8.27E-08	***
		Zone × Density	8, 28	16.02	1.40E-08	***
Individual reproduction	None	Zone	2, 28	89.077	7.27E-13	***
		Density	4, 28	36.389	1.03E-10	***
		Zone × Density	8, 28	20.895	6.92E-10	***
Relative Interaction Index	ART	Zone	2, 28	14.94	3.84E-05	***
		Density	4, 28	25.59	5.34E-09	***
		Zone × Density	8, 28	2.06	0.0754	ns
Survival rate	None	Zone	2, 30	0.79	0.4639	ns
		Density	4, 30	3.26	0.0248	*
		Zone × Density	8, 30	1.57	0.1760	ns
Population biomass (g/m^2)	Log	Zone	2, 28	30.52	9.24E-08	***
		Density	4, 28	2.07	0.1121	ns
		Zone × Density	8, 28	1.61	0.1665	ns
	Log	Zone	2, 28	23.79	9.19E-07	***

Population reproduction (seeds/m²)	Density	4, 28	1.15	0.3541	ns
	Zone × Density	8, 28	1.36	0.2576	ns